

# Linking transitions in the $A \approx 80$ region of superdeformation

C J Chiara<sup>1</sup>, D G Sarantites<sup>1</sup>, M Montero<sup>1</sup>, J O'Brien<sup>1</sup>, W Reviol<sup>1</sup>,  
O L Pechenaya<sup>2</sup>, R M Clark<sup>3</sup>, P Fallon<sup>3</sup>, A G3rgen<sup>3</sup>, A O Macchiavelli<sup>3</sup>,  
D Ward<sup>3</sup>, W Satuła<sup>4</sup> and Y R Shimizu<sup>5</sup>

<sup>1</sup> Chemistry Department, Washington University, St. Louis, MO 63130, USA

<sup>2</sup> Physics Department, Washington University, St. Louis, MO 63130, USA

<sup>3</sup> Nuclear Science Division, Lawrence Berkeley National Laboratory, Berkeley, CA 94720, USA

<sup>4</sup> Institute of Theoretical Physics, Warsaw University, Hoża 69, PL-00681, Warsaw, Poland

<sup>5</sup> Department of Physics, Kyushu University, Fukuoka 812-8581, Japan

E-mail: [cjc@wustl.edu](mailto:cjc@wustl.edu)

Received 5 August 2005

Accepted for publication 1 September 2005

Published 28 June 2006

Online at [stacks.iop.org/PhysScr/T125/119](http://stacks.iop.org/PhysScr/T125/119)

## Abstract

In a recent study of superdeformed (SD) bands in the  $A \approx 80$  region, three discrete linking transitions to states of normal deformation (ND) were identified in  $^{84}\text{Zr}$ . The properties of the abrupt decay out of the SD well in  $^{84}\text{Zr}$  are compared with those in other SD mass regions. Several theoretical calculations suggest that there is extensive mixing of configurations in the SD and ND minima and very little potential barrier between the two wells, leading to a rapid, highly fragmented decay-out process.

PACS numbers: 23.20.Lv, 27.50.+e

## 1. Introduction

Superdeformed (SD) bands have been observed in several distinct mass regions spanning the nuclear chart [1]. In the majority of these cases, discrete  $\gamma$  transitions linking the SD sequences to states of normal deformation (ND) have not been identified. Without such links, the interpretations for these bands rely primarily on  $\mathcal{J}^{(2)}$  moments of inertia and (in some cases)  $Q_t$  transition quadrupole moments, while the spins, parities, and excitation energies can only be estimated. Thus, the observation of links is of vital importance in studying the SD phenomenon. In addition to pinning down the above quantities which provide tests of the models, it may also permit a study of the decay mechanism itself.

SD bands generally share a common feature in that the intensity remains within a second, highly deformed potential minimum until a given spin is reached, upon which the band rapidly depopulates to the first minimum over just a few states. There are considerable differences, however, when one examines the detailed properties of the decay out in different mass regions.

In table 1, a representative nucleus is given from each of the major SD regions in which links have been observed. It is worth noting that the nature of the observed decay out (fifth

column) is quite different for the various mass regions. For example, in the  $A \approx 40$  region, the decay tends to proceed via intense E2 transitions, due to strong mixing of a small number of configurations. Most of the decay-out intensity ( $\Sigma I_{\text{out}}$  in column 6 of the table) is observed in this case [2, 4, 14]. In the  $A \approx 150$  and 190 regions, on the other hand, the observed links carry only a small fraction of the SD intensity, and generally include weak, statistical E1 decays [10, 12, 15, 16]. In the  $A \approx 60$  and 130 regions, the excited shapes are not as deformed as in the other regions (third column of table 1), and it has been found that the first and second potential minima are not well separated by any significant barrier [6, 17]. Here, a sizable fraction of the decay-out intensity  $\Sigma I_{\text{out}}$  is observed. The  $A \approx 130$  SD nuclei tend to decay out nearer the yrast line than found in other regions; this is indicated in column 4 of the table by the small values of  $\Delta E_x$ , the difference in excitation energy (at decay-out spins) between the SD and yrast ND states with the same spin and parity. The  $A \approx 60$  SD nuclei are unique in that, in some cases, prompt proton or  $\alpha$ -particle decay is also observed from the SD well to spherical states in the daughter nuclei, in competition with the discrete  $\gamma$  decays to ND states in the same nucleus [7, 18, 19]. Clearly, there are diverse possibilities for available SD decay modes. It continues to be a challenge to develop

**Table 1.** Overview of the decay properties of yrast SD bands in representative nuclei for various mass regions. The quadrupole deformation parameter  $\beta_2$  deduced from measured  $Q_t$  values is given in the third column. The energy difference  $\Delta E_x$  is between SD states for which discrete decay out has been observed and the yrast (ND) state with the same spin and parity; the range over several SD states is given. The total *observed* decay-out intensity is given by  $\Sigma I_{\text{out}}$ , relative to the maximum intensity of the SD band. The last column gives remarks related to the discussion below. The deformation for  $^{40}\text{Ca}$  is valid for the high-spin regime; admixtures with ND configurations reduce  $\beta_2$  to 0.4 at low spin [2]. The deformation for  $^{84}\text{Zr}$  was determined in [3]; the remaining information for this nucleus is from the current study.

A	Nuclide	$\beta_2$	$\Delta E_x$ (MeV)	Dominant decay mode(s)	$\Sigma I_{\text{out}}$	Remarks
40	$^{40}\text{Ca}$ [4, 2]	0.58 <sup>a</sup>	1.0–1.8	Intense E2 $\gamma$ rays	$\sim 100\%$	Strong SD-ND mixing
60	$^{59}\text{Cu}$ [5, 6, 7]	0.41	1.1	E2 $\gamma$ rays; prompt particles	$\sim 100\%$	Small barriers
80	$^{84}\text{Zr}$ [3]	0.56	2.8	Weak E1 $\gamma$ rays	$\sim 2\%$	Statistical decay
130	$^{134}\text{Nd}$ [8, 9]	0.35	0.3–0.6	E1 $\gamma$ rays	$\sim 51\%$	Small barriers
150	$^{152}\text{Dy}$ [10, 11]	0.69	2.6–3.0	Weak E1 $\gamma$ rays	$\sim 2\%$	Statistical decay
190	$^{194}\text{Hg}$ [12, 13]	0.49	4.1–4.4	Weak E1 $\gamma$ rays	$\sim 4\%$	Statistical decay

<sup>a</sup>At high spins.

a unifying model that can reproduce these properties for SD bands in general.

The  $A \approx 80$  SD region has been extensively studied, with over 30 bands observed in more than a dozen nuclei, and many with subsequent  $Q_t$  measurements having been performed [1, 3]. Yet prior to the current study, none of these bands had been linked. In this presentation, we give the decay-out properties of the newly linked yrast SD band in  $^{84}\text{Zr}$ , and show how it compares with the properties of SD nuclei in other mass regions.

## 2. Experimental details

High-spin states in  $^{84}\text{Zr}$  were populated via the  $^{58}\text{Ni}(^{32}\text{S}, \alpha 2p)$  reaction. A 140 MeV  $^{32}\text{S}$  beam, provided by the 88" Cyclotron at Lawrence Berkeley National Laboratory, was directed on to a self-supporting  $0.50 \text{ mg cm}^{-2}$   $^{58}\text{Ni}$  target. The Gammasphere [20] and Microball [21] arrays were used to detect  $\gamma$  rays and charged particles, respectively. Gammasphere consisted of 102 Compton-suppressed HPGe detectors arranged in 16 rings of constant azimuthal angle relative to the beam. A total of  $2.2 \times 10^9$  events with  $\gamma$ -ray fold five or higher were recorded, along with any correlated Microball pulse-height and timing information. The efficiencies for detecting protons and  $\alpha$  particles were  $\varepsilon_p \approx 80\%$  and  $\varepsilon_\alpha \approx 70\%$ , respectively. Events were selected offline which included exactly one  $\alpha$  particle and one or two protons. A total of  $402 \times 10^6$  such events were unfolded into constituent threefold  $\gamma$  coincidences for subsequent analysis.

## 3. Results

The current work confirms the  $^{84}\text{Zr}$  SD and ND decay schemes deduced by, respectively, Jin *et al* [22] and Cardona *et al* [23]. The yrast SD band (SD1) comprises nine transitions; their energies are listed in the first column of table 2. Double gates were placed on pairs of these  $\gamma$  rays in band SD1. The spectrum resulting from the sum of all possible double gates in this band is shown in figure 1. Several high-energy ( $>3 \text{ MeV}$ ) transitions were revealed to be in coincidence with members of the SD band. Three of them, with energies 3464, 3743 and 4052 keV (see bottom of table 2 and inset of figure 1), are identified as decay-out transitions. Spectra formed by double gating on each of these transitions and the members of band SD1 show the coincident

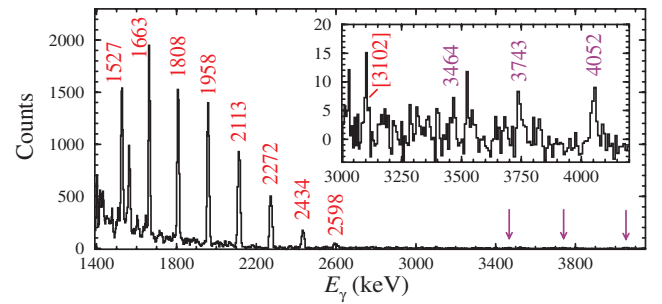


**Figure 1.** Spectrum formed by the sum of all double gates on transitions within band SD1. Peaks are labelled with their energies in keV. The arrows mark the energies of the linking transitions. The inset shows a magnified view of this high-energy region. The 3102 keV peak corresponds to a transition observed feeding into the SD band.

transitions in SD1 clearly, as well as transitions in the ND part of the decay scheme. Each of the linking transitions is in coincidence with a different ND structure: 4052, 3743 and 3464 keV with the positive-parity ground-state band, a negative-parity band, and a positive-parity side band, respectively. Energy sums and coincidence relations are consistent with the placement of the 4052, 3743 and 3464 keV  $\gamma$  rays decaying out of the lowest observed state of band SD1 into the  $24^+$ ,  $24^-$  and  $(24^+)$  states of these three ND bands. Thus, these are single-step linking transitions between the SD and ND wells of  $^{84}\text{Zr}$  which fix the excitation energies of the states in band SD1. The state energies are given in the second column of table 2.

The intensity of band SD1 ( $I_{\text{SD1}}$ ) is about 3% that of the  $2^+ \rightarrow 0^+$  540 keV transition. Of this, only about 2% of the  $I_{\text{SD1}}$  intensity passes through the three linking transitions ( $\Sigma I_{\text{out}} \approx 0.02 I_{\text{SD1}}$ ). The remaining 98% of the SD1 decay has not been identified in this analysis. Fractions of this intensity are probably carried by additional high-energy transitions that could not be placed in the level scheme, such as those found in the inset of figure 1, or by even weaker (quasi-continuum) transitions that are not resolved from background.

The multipolarities of the 4052 and 3743 keV linking transitions were determined to be  $\Delta I = 1$  E1 and E2/M1, respectively, through a standard angular-correlation analysis. The distinction between electric and magnetic character cannot be made directly in such an analysis; however, the observations that the 3743 keV transition is mixed and the 4052 keV transition is pure dipole, and that these two

**Table 2.** Properties of the  $\gamma$  rays within and depopulating the yrast SD band in  $^{84}\text{Zr}$ . The excitation energies  $E_{x,i}$  for the initial state for each transition is given in the second column. The last column gives the  $\gamma$ -ray intensities normalized to 100 for the 540 keV  $2^+ \rightarrow 0^+$  ground-state transition.

$E_\gamma$ (keV)	$E_{x,i}$ (keV)	$I_i^\pi \rightarrow I_f^\pi$	$\sigma\lambda$	$I_\gamma$
2780	36874	$43^- \rightarrow 41^-$	E2	0.007
2598	34094	$41^- \rightarrow 39^-$	E2	0.03
2434	31496	$39^- \rightarrow 37^-$	E2	0.17
2272	29062	$37^- \rightarrow 35^-$	E2	0.57
2113	26790	$35^- \rightarrow 33^-$	E2	1.29
1958	24677	$33^- \rightarrow 31^-$	E2	2.09
1808	22718	$31^- \rightarrow 29^-$	E2	2.69
1663	20910	$29^- \rightarrow 27^-$	E2	2.76
1527	19247	$27^- \rightarrow 25^-$	E2	1.80
3464	17721	$25^- \rightarrow (24^+)^a$	(E1)	0.012
3743	17721	$25^- \rightarrow 24^{-a}$	M1/E2	0.020
4052	17721	$25^- \rightarrow 24^{+a}$	E1	0.025

<sup>a</sup>These decays are to ND states.

transitions feed states of opposite parities, make the above assignment the favoured one (compared to having an unlikely mixed-M2/E1 assignment). The lowest observed state in band SD1 is thus assigned  $I^\pi = 25^-$ . The spins and parities of the SD states are given in column 3 of table 2.

#### 4. Discussion

The observed decay intensity  $\Sigma I_{\text{out}}$  for band SD1 of  $^{84}\text{Zr}$  is rather small, as is also seen in the  $A \approx 150$  and 190 SD regions (see table 1). These latter cases have been analysed in several studies by a variety of statistical-decay models (see [24] and references therein). In particular, band SD1 in  $^{84}\text{Zr}$  and the yrast SD band in  $^{152}\text{Dy}$  [10] share several common features: they both decay out at similar  $\Delta E_x$ ; the decay proceeds through very weak ( $\sim 1\%$  intensity,  $B(\text{E}1) \sim 10^{-6}$  W.u.) E1 transitions; and the decay out is from SD states near  $25\hbar$ . This is quite different from the intense decays observed around  $A \approx 40$  and 60, where a few strong E2 transitions connect the SD and ND bands, and the decay occurs at fairly low spins (see, e.g. [4, 18]). The similarity between  $^{84}\text{Zr}$  and  $^{152}\text{Dy}$  suggests that a related statistical-decay model approach can be used here as well.

We follow the purely statistical formalism presented in [25], using the same parameterization as used in the study in [26]. This model is used to determine the spreading width  $\Gamma^\downarrow$ , which is a measure of the mixing between the SD and the ND wells, as a function of the parameters  $\Gamma_S$ ,  $\Gamma_N$ ,  $d$  and  $F_S$ .

The  $\Gamma_S$  and  $\Gamma_N$  parameters are the decay widths in the SD and ND wells, respectively. The former can be determined by a direct measurement of the lifetimes (or, equivalently, the  $Q_t$  moment) in the SD band. The latter has two components,  $\Gamma_N = \Gamma_N^{\text{E}2} + \Gamma_N^{\text{E}1}$ . The collective E2 contribution is estimated for the ND states similarly to the SD decay width. The statistical E1 contribution is an estimate related to the Fermi gas density of states and the GDR strength function; specifically, it takes the approximate form

$$\Gamma_N^{\text{E}1} = 3.45 \times 10^{-6} N Z A^{1/3} \left( \frac{U}{a} \right)^{5/2},$$

**Table 3.** Fraction  $F_S$  of intensity remaining in SD band at each state, spreading width  $\Gamma^\downarrow$  deduced using the formalism of [25], and  $B(\text{E}1)$  strength of linking transitions. Apart from the results for  $^{84}\text{Zr}$ , the  $\Gamma^\downarrow$  values are reproduced from [24]. The  $B(\text{E}1)$  strengths are from [16] ( $^{192}\text{Pb}$ ), [15] ( $^{194}\text{Pb}$ ), [12] ( $^{194}\text{Hg}$ ), [10] ( $^{152}\text{Dy}$ ) and the current work for  $^{84}\text{Zr}$ .

Nuclide	$I^\pi$	$F_S$	$\Gamma^\downarrow$ (eV)	$B(\text{E}1)$ (W.u.)
$^{192}\text{Pb}$	$8^+$	$<0.25$	$>510$	—
	$10^+$	0.12	7509	$5 \times 10^{-7}$
$^{194}\text{Pb}$	$6^+$	$<0.04$	$>100$	$4 \times 10^{-8}$
	$8^+$	0.65	0.223	$2 \times 10^{-8}$
$^{194}\text{Hg}$	$10^+$	$<0.05$	$>2.12$	$7 \times 10^{-9}$
	$12^+$	0.58	0.058	$7 \times 10^{-9}$
$^{152}\text{Dy}$	$28^+$	0.6	6	$2 \times 10^{-6}$
$^{84}\text{Zr}$	$25^-$	$<0.2$	$>3700$	$5 \times 10^{-6}$
	$27^-$	0.65	273	—

giving  $\Gamma_N^{\text{E}1}$  in eV when  $U$  and  $a^{-1}$  are in MeV. Here, the level-density parameter  $a = A/8.5$  MeV has been used, as in [26], and no backshift has been subtracted from the energy for this nucleus, i.e.  $U = \Delta E_x$ .

The average ND level spacing  $d$  is taken as the reciprocal of the Fermi gas density of states in the ND well, namely

$$d(U)^{-1} = \rho(U) = \frac{\sqrt{\pi} a \exp(2\sqrt{aU})}{48 (aU)^{5/4}}.$$

Finally,  $F_S$  is the fraction of the intensity remaining within the SD band at the state of interest.

Using the formalism of [25], a value of  $\Gamma^\downarrow > 3.7$  keV is estimated for the  $25^-$  SD state in  $^{84}\text{Zr}$ . This is a lower limit because only an upper limit on  $F_S$  is known—there are no in-band SD decays observed parallel to the linking transitions. This value is several orders of magnitude larger than in  $^{152}\text{Dy}$  or in several of the  $A \approx 190$  cases, as shown in table 3. This suggests that there is extensive mixing between configurations in the SD and ND wells in  $^{84}\text{Zr}$ . The last column of table 3 gives the deduced  $B(\text{E}1)$  strengths, where available. It is perhaps surprising that the  $B(\text{E}1)$  strengths for  $^{84}\text{Zr}$  and  $^{152}\text{Dy}$  are rather similar despite the large difference in  $\Gamma^\downarrow$ .

A large value for  $\Gamma^\downarrow$  may be a reflection of the height of the barrier separating the SD and ND wells. Calculations using a Nilsson potential with static and dynamic pairing correlations included [27] reveal the following. The well-confined SD minimum at high spins quickly spreads in deformation space as spin decreases, becoming a broad, shallow minimum that extends into ND shapes. At low spins, there is no longer a well-defined barrier. Details of this analysis will be presented elsewhere [28].

We have also performed Skyrme–Hartree–Fock calculations at a constrained spin of  $\langle I \rangle = 25\hbar$ , and find there are many configurations at different deformations coexisting at similar excitation energies. This seems consistent with the above picture of a broad, shallow potential spreading across SD and ND shapes, and allowing the possibility of extensive mixing of multiple configurations. This mixing then enhances the decay out through many weak transitions.

#### 5. Conclusion

The yrast SD band in  $^{84}\text{Zr}$  was recently linked to states in the ND well, allowing the determination of the spins,

parity, and excitation energies of the SD states. The linking transitions were found to be rather weak dipole transitions, much like those observed in the  $A \approx 150$  and 190 regions. The spreading width, however, is considerably larger for  $^{84}\text{Zr}$  than most of these other examined cases, suggesting extensive mixing of SD and ND states. This conclusion is supported by calculations of the potential barrier and constrained-spin Skyrme–Hartree–Fock calculations.

### Acknowledgments

This work was supported in part by the US Department of Energy under grant no DE-FG02-88ER-40406 and contract no DE-AC03-76SF-00098, and the Polish Committee for Scientific Research, contract no 1 P03B 059 27.

### References

- [1] Singh B, Zywna R and Firestone R B 2002 *Nucl. Data Sheets* **97** 241
- [2] Chiara C J *et al* 2003 *Phys. Rev. C* **67** 041303(R)
- [3] Lerma F *et al* 2003 *Phys. Rev. C* **67** 044310
- [4] Ideguchi E *et al* 2001 *Phys. Rev. Lett.* **87** 222501
- [5] Andreoiu C *et al* 2000 *Phys. Rev. C* **62** 051301(R)
- [6] Andreoiu C *et al* 2003 *Phys. Rev. Lett.* **91** 232502
- [7] Rudolph D *et al* 2002 *Phys. Rev. Lett.* **89** 022501
- [8] Petrache C M *et al* 1996 *Phys. Rev. Lett.* **77** 239
- [9] Petrache C M *et al* 1998 *Phys. Rev. C* **57** R10
- [10] Lauritsen T *et al* 2002 *Phys. Rev. Lett.* **88** 042501
- [11] Savajols H *et al* 1996 *Phys. Rev. Lett.* **76** 4480
- [12] Khoo T L *et al* 1996 *Phys. Rev. Lett.* **76** 1583
- [13] Dewald A *et al* 2001 *Phys. Rev. C* **64** 054309
- [14] Svensson C E *et al* 2000 *Phys. Rev. Lett.* **85** 2693
- [15] Hauschild K *et al* 1997 *Phys. Rev. C* **55** 2819
- [16] Wilson A N *et al* 2003 *Phys. Rev. Lett.* **90** 142501
- [17] Svensson C E *et al* 1997 *Phys. Rev. Lett.* **79** 1233
- [18] Afanasjev A V and Ragnarsson I 1996 *Nucl. Phys. A* **608** 176
- [19] Rudolph D *et al* 1998 *Phys. Rev. Lett.* **80** 3018
- [20] Rudolph D *et al* 1999 *Phys. Rev. Lett.* **82** 3763
- [21] Rudolph D *et al* 2001 *Phys. Rev. Lett.* **86** 1450
- [22] Lee I Y 1990 *Nucl. Phys. A* **520** 641c
- [23] Sarantites D G *et al* 1996 *Nucl. Instrum. Methods Phys. Res. A* **381** 418
- [24] Jin H-Q *et al* 1995 *Phys. Rev. Lett.* **75** 1471
- [25] Cardona R *et al* 2003 *Phys. Rev. C* **68** 024303
- [26] Wilson A N, Sargeant A J, Davidson P M and Hussein M S 2005 *Phys. Rev. C* **71** 034319
- [27] Gu Jian-zhong and Weidenmüller H A 1999 *Nucl. Phys. A* **660** 197
- [28] Wilson A N 2004 *Prog. Theor. Phys. (Kyoto)* (Suppl.) **154** 138
- [29] Method is described in Shimizu Y R, Vigezzi E, Døssing T and Broglia R A 1993 *Nucl. Phys. A* **557** 99c
- [30] Chiara C J *et al* 2006 *Phys. Rev. C* **73** 021301(R)